INTERNATIONAL JOURNAL OF

MEDICAL BIOCHEMISTRY

DOI: 10.14744/ijmb.2025.32656 Int J Med Biochem 2025;8(4):282–291

Research Article



Adaptive mitochondrial modules: Going with the flow of cancer-specific metabolic rewiring

Mehmet Taha Yildiz

Department of Child Development, University of Health Sciences, Hamidiye Faculty of Health Sciences, Istanbul, Türkiye

Abstract

Objectives: Mitochondrial gene networks constitute a fundamental subsystem of cellular homeostasis, integrating bioenergetic, metabolic, and signaling functions. In cancer, the rewiring of these networks represents a critical mechanism of metabolic adaptation, enabling tumor cells to sustain growth and survival under diverse microenvironmental constraints. To systematically characterize these alterations, we analyzed transcriptomic data from The Cancer Genome Atlas (TCGA) with a specific focus on mitochondrial genes, aiming to uncover cancer-type-specific patterns of differential expression and their potential biological implications.

Methods: Transcriptomic data from The Cancer Genome Atlas (TCGA) were analysed to identify differential expression patterns in mitochondrial genes. Weighted Gene Co-expression Network Analysis (WGCNA) was applied to detect co-expressed gene modules. The biological relevance of these modules was assessed through functional enrichment analysis and survival modelling using Cox regression and Kaplan–Meier estimations. Dimensionality reduction techniques including PCA and UMAP were used to evaluate module-driven clustering patterns across cancer types.

Results: Seven mitochondrial gene modules were identified, six of which demonstrated significant associations with specific cancer types. Modules ME2, ME4, ME5, ME6, and ME7 were associated with improved overall survival, while ME3 correlated with poorer prognosis. Functional enrichment analyses revealed distinct mitochondrial processes including oxidative phosphorylation, apoptosis, fatty acid β -oxidation, and ketone body metabolism. Dimensionality reduction analyses supported the presence of module-specific expression patterns with cancer-type-dependent clustering.

Conclusion: The observed cancer-type-specific expression and prognostic associations of mitochondrial gene networks reflect their central involvement in the metabolic flexibility of tumors. By underscoring the clinical and biological significance of mitochondrial subsystems, these findings suggest that they may serve not only as prognostic markers but also as promising targets for therapeutic modulation.

Keywords: Cancer metabolism, co-expression modules, gene expression profiling, gene co-expression networks, mitochondrial genes, systems biology

How to cite this article: Yildiz MT. Adaptive mitochondrial modules: Going with the flow of cancer-specific metabolic rewiring. Int J Med Biochem 2025;8(4):282–291.

Biological systems are intrinsically complex, dynamic, and deeply interconnected. To maintain cellular homeostasis, they rely on multilayered regulatory networks that combine structural redundancy with exceptional adaptive flexibility [1, 2]. This adaptability may allow cancer cells to emerge as reorganized—yet still coordinated—deviations from the original regulatory architecture. Even in the disease state, internal logic

and systemic coordination may persist through altered but non-random arrangements of regulatory configurations [3].

Understanding these transformations is particularly challenging due to the high-dimensional, non-linear, and interdependent nature of molecular interactions. Numerous molecular components operate simultaneously and influence one another in non-linear ways, making it difficult to isolate individual

Address for correspondence: Mehmet Taha Yildiz, MD. Department of Child Development, University of Health Sciences, Hamidiye Faculty of Health Sciences, Istanbul, Türkiye

Phone: +90 554 227 43 48 E-mail: mtaha.yildiz@sbu.edu.tr ORCID: 0000-0003-4768-0333

Submitted: July 11, 2025 **Revised:** September 02, 2025 **Accepted:** September 03, 2025 **Available Online:** October 21, 2025 **OPEN ACCESS** This is an open access article under the CC BY-NC license (http://creativecommons.org/licenses/by-nc/4.0/).





effects or predict system-wide behavior. This complexity poses significant challenges for both computational modeling and biological interpretation, especially when attempting to capture the emergent properties of the system as a whole [4–6].

One rational strategy to navigate this complexity is to focus on key functional groups of genes or proteins (regulatory nodes) that coordinate specific biochemical pathways or molecular processes. These groups are critical for cellular survival and proliferation and may be maintained or repurposed by cancer cells to sustain viability, differentiation, and growth [7, 8]. Among these, mitochondria are pivotal due to their roles in metabolic reprogramming, redox signaling, and apoptotic regulation [9]. Beyond these functions, while mitochondrial functions are modulated by nuclear-encoded proteins (1,138 genes), their compact genome (37 genes), defined metabolic pathways, and membrane-bound localization render them a relatively self-contained and tractable subsystem for dissecting cancer's regulatory rewiring [10–14].

Given these considerations, we hypothesize that differential mitochondrial gene expression patterns can reveal cancer-type-specific prognostic modules. Their regulatory roles are not fixed but dynamically adapted to meet the context-specific demands of diverse tumor types. This plasticity may underlie resistance to single-agent therapies, as tumors exploit the flexibility of these mitochondrial subsystems—groups of interacting genes or proteins performing coordinated functions—to sustain survival under therapeutic pressure [15–20].

In this study, we adopt a systems biology approach to investigate mitochondrial gene networks as a model regulatory subsystem—a group of interacting genes or proteins that jointly perform a functional role. Our aim is to identify adaptive mitochondrial modules that contribute to cancer-type-specific regulatory reorganization, with a particular focus on their prognostic significance and functional diversity across tumors.

Materials and Methods

Ethical considerations

This study was conducted exclusively using publicly available data from The Cancer Genome Atlas (TCGA) project (https:// www.cancer.gov/tcga). All data were fully deidentified and used in accordance with the TCGA publication guidelines and data access policies. No new human or animal data were collected or generated by the authors. Therefore, this research is exempt from institutional review board (IRB) approval under current regulations [21]. All procedures performed in this study complied with the ethical standards of the TCGA consortium and with the 1964 Helsinki Declaration and its later amendments. The study complies with the U.S. Department of Health and Human Services policy for the protection of human research subjects (45 CFR 46). The TCGA provides an invaluable and ethically curated resource for studying cancer biology at the molecular level, enabling reproducible and large-scale in silico analyses [22, 23].

Study design and overview

To investigate mitochondrial gene regulatory networks across diverse cancer types, we used a systems biology framework that combines co-expression network analysis, module—phenotype association, and mechanistic enrichment. Our middle-out strategy—anchored at the module level where eigengenes represent the dominant expression pattern of co-expressed genes—links gene-level perturbations to higher-order phenotypes. This design enables the detection of biologically meaningful modules first and their subsequent association with phenotypes, balancing molecular detail with system-level interpretation.

This integrative analysis was conducted in three key phases; first, we analysed RNA-seq data from TCGA to identify tumor-specific co-expression modules (Fig. 1, steps 1 to 3). Second, we correlated these modules with clinical outcomes including survival and molecular subtypes (Fig. 1, steps 4 to 6). Third, we performed pathway enrichment analysis using pathway enrichment results obtained via Enrichr-KG which integrates GO, KEGG and Reactome databases to annotate mechanistic functions (Fig. 1, step 7) [24]. This integrative strategy enabled systematic mapping of mitochondrial regulatory programs in cancer while maintaining biological interpretability.

Data acquisition and preprocessing

RNA-seq data and clinical metadata were retrieved from TCGA using the GDCRNATools R package [25]. Raw HTSeq count data and corresponding clinical metadata were downloaded for 23 cancer types. Only cancer types with ≥ 2 matched Solid Tissue Normal samples were retained, excluding other tissue types and technical duplicates. This filtering yielded 17 cancer types: BLCA, BRCA, CESC, COAD, ESCA, GBM, HNSC, KICH, KIRC, KIRP, LIHC, LUAD, PRAD, READ, STAD, THCA, UCEC. Normalization was performed using the Trimmed Mean of M-values (TMM) method, followed by voom transformation, as implemented in the GDCRNATools package. Only genes annotated as mitochondrial in the MitoCarta3.0 [26] human gene set (n=1,138) were included, resulting in expression profiles for 7,874 samples (7,202 Primary Tumor, 672 Solid Tissue Normal). Sample counts per cancer type ranged from 91 (KICH) to 1,208 (BRCA).

Delta expression matrix calculation

To quantify tumor-specific transcriptional alterations, a delta expression matrix was constructed by subtracting the mean expression of each gene in Solid Tissue Normal samples from Primary Tumor expression values, separately within each cancer type. Sample types were assigned using clinical metadata. The final matrix contained 1,138 mitochondrial genes (rows) and 7,202 tumor samples (columns). All identifiers were checked for dimensional consistency prior to further analysis. A limitation of this approach is the small number of normal samples in a few cancer types, which may reduce the robustness of the differential expression scores.

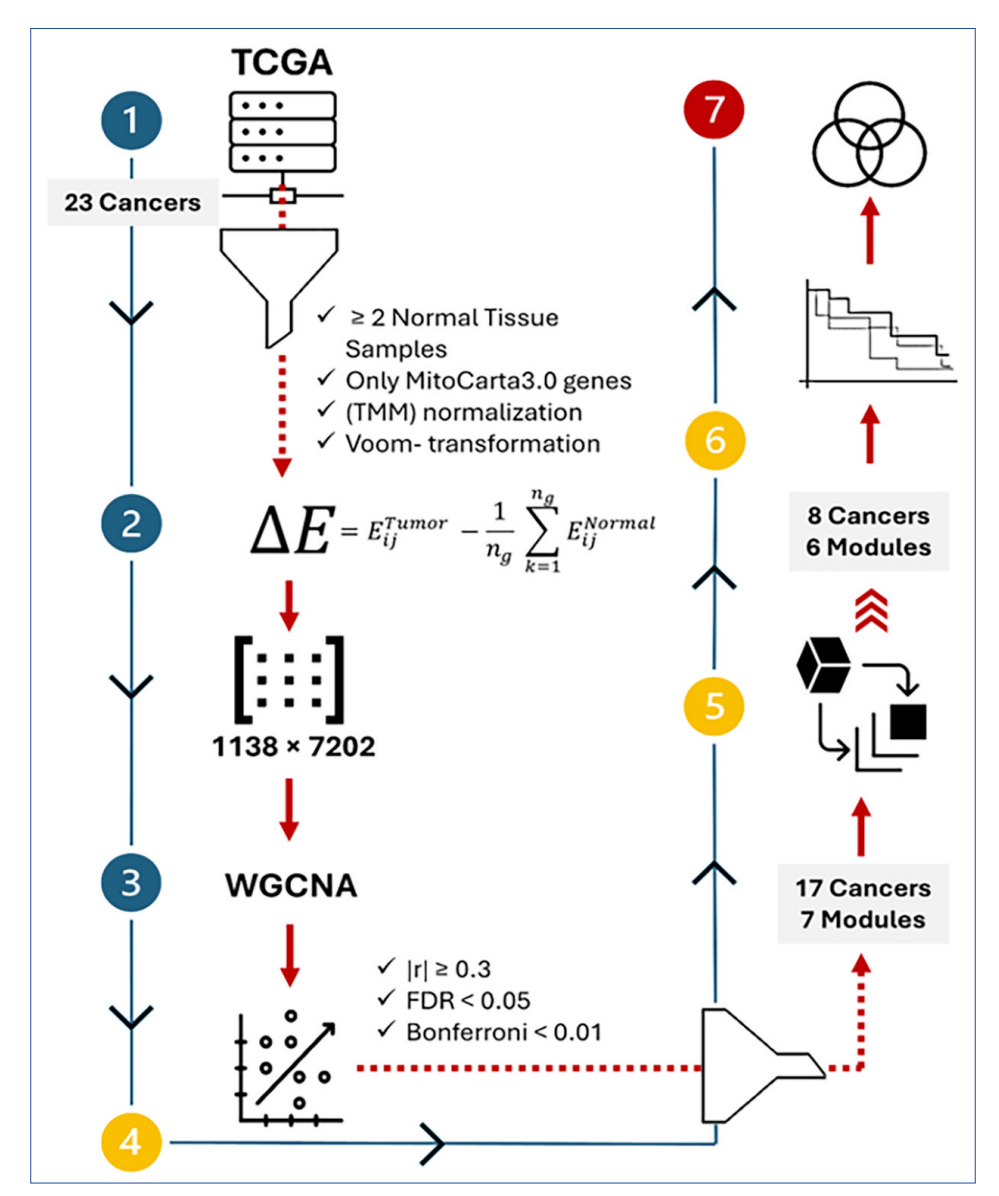


Figure 1. Schematic overview of the module-based cancer analysis pipeline. The workflow consists of seven main steps: (1) acquisition and preprocessing of gene expression and phenotype data, (2) calculation of delta expression, (3) construction of a gene co-expression network and module detection via WGCNA tool, (4) correlation analysis between modules and cancer types, (5) dimensionality reduction and visualization of module-trait relationships, (6) survival analysis based on module expression, and (7) functional enrichment analysis to infer biological relevance. Funnel icons represent filtering steps, with specific exclusion criteria indicated adjacent to each filter. WGCNA: Weighted Gene Co-expression Network Analysis.

Co-expression network construction and module detection

Weighted Gene Co-expression Network Analysis (WGCNA) was performed on the delta expression matrix to identify modules of co-expressed mitochondrial genes [27]. A soft-thresholding power of β =4 was selected based on scale-free topology and mean connectivity criteria (R^2 =0.89), as illustrated in Appendix 1a-b. The resulting adjacency matrix was used to compute the topological overlap matrix (TOM), followed by hierarchical clustering and dynamic tree cutting, which identified seven distinct co-expression modules (Appendix 1c).

To evaluate module stability, the dataset was randomly split into reference (70%) and test (30%) subsets, and module preservation was assessed across 20 permutations using both Z-summary and median rank statistics, with higher Z-summary and lower median rank values indicating stronger and more biologically coherent preservation; median rank values supported the hierarchy suggested by Z-summary, hub genes were identified based on intra-module connectivity (Appendix 2). The Topological Overlap Matrix (TOM) was used to compute kWithin values, and genes with kWithin >1 SD above the

module mean were designated as hub genes. These genes were retained for downstream functional analyses.

Module-cancer type correlation analysis

Cancer type metadata was one-hot encoded to match the sample order in the module eigengene (ME) matrix. Pearson correlations between MEs and binary cancer-type variables were computed to identify module—cancer associations, with significance assessed via Student's t-distribution. Multiple testing correction was performed using both False Discovery Rate (FDR) and Bonferroni methods. Correlations with $|r| \ge 0.3$ and adjusted p-values <0.05 and FDR<0.01 (Bonferroni) were considered significant (Appendix 2).

Dimensionality reduction and visualization of moduletrait relationships

To explore module–cancer associations, dimensionality reduction was applied to delta expression data restricted to genes within significant modules. Principal Component Analysis (PCA) was used to project samples into lower-dimensional space while preserving variance. Clustering patterns by cancer type were visualized along the first two principal components, and cluster quality was assessed using silhouette scores. To capture nonlinear structure, UMAP and t-SNE were also performed, both supporting PCA-derived groupings and revealing distinct cancer type separations based on module gene expression.

Functional enrichment analysis

Functional enrichment analysis was conducted for each module using the Enrichr-KG platform, which integrates curated databases such as WikiPathways, Reactome, KEGG, and Gene Ontology [24]. Enrichment was based on the statistical overrepresentation of module genes within known pathways, assessed via adjusted p-values. Only modules significantly correlated with cancer types were included to focus on biologically relevant gene networks. Significant terms were summarized and visualized to aid interpretation of predominant functional themes within each module.

Survival analysis

The prognostic relevance of mitochondrial gene co-expression modules was assessed using Kaplan-Meier survival curves and univariate Cox proportional hazards models based on module eigengene expression. Module scores were matched with clinical survival data (time-to-event and event status) from 7,202 tumor samples with complete metadata. Samples were dichotomized into "High" and "Low" groups by the median eigengene value per module. While median-based grouping is common practice, it may lead to some information loss, which should be considered when interpreting results. Survival differences were evaluated with log-rank tests, and hazard ratios (HR) with 95% confidence intervals were estimated via Cox models. P-values were adjusted for multiple testing using the Benjamini-Hochberg false discovery rate (FDR) method (Appendix 2). This approach provided robust prognostic assessment across cancer types while avoiding assumptions related to continuous variable modeling.

Table 1. Mitochondrial gene co-expression modules and preservation statistics

| Module | Gene count | Z -summary | Median rank |
|--------|------------|-------------------|-------------|
| ME1 | 443 | 28.85 | 2 |
| ME3 | 107 | 16.54 | 4 |
| ME2 | 162 | 13.89 | 7 |
| ME4 | 99 | 13.29 | 5 |
| ME6 | 58 | 12.27 | 2 |
| ME5 | 72 | 10.13 | 5 |
| ME7 | 46 | 9.85 | 4 |

Preservation was assessed using Z-summary, a composite statistic reflecting module stability across datasets, and median rank metrics over 20 permutations. Higher Z-summary and lower median rank values indicate stronger and more biologically coherent module preservation across cancer types.

Software and tools

All analyses were performed using R version 4.4.1 (2024-06-14) on Windows 11 x64. Key R packages included GDCRNATools (v1.18.0), WGCNA (v1.73), survival (v3.8-3), survminer (v0.5.0), dynamicTree-Cut (v1.63-1), fastcluster (v1.2.6), ggplot2 (v3.5.2), ggpubr (v0.6.0), tidyverse (v2.0.0), umap (v0.2.10.0), and Rtsne (v0.17).

Results

Module preservation and structural robustness

WGCNA identified seven mitochondrial gene co-expression modules (ME1–ME7), ranging from 46 to 443 genes in size (Table 1). Genes not assigned to any module (ME0) were grouped into the gray module and excluded from downstream analyses. Module preservation was evaluated using Z-summary and median rank statistics across 20 permutations. Four modules—ME1, ME3, ME2, and ME4—showed strong preservation. ME6 and ME5 also met the threshold for high preservation, while ME7 demonstrated moderate stability. Median rank values supported the Z-summary-based hierarchy of module robustness. Collectively, these results indicate that the identified modules represent reproducible and biologically coherent co-expression structures among mitochondrial genes across cancer types.

Module-cancer type associations

To evaluate the biological relevance of mitochondrial gene modules across cancer types, we assessed the correlations between module eigengenes and tumor labels. Six of the seven modules (ME2–ME7) showed statistically significant associations with at least one cancer type (Fig. 2). In total, twelve significant module–cancer type pairs were identified, involving eight distinct cancer types. Full correlation coefficients and adjusted p-values are presented in Table 2. The strongest positive associations were observed for ME6 with KIRC and ME5 with THCA, while ME7 exhibited the most pronounced negative correlation with LIHC.

These findings suggest that mitochondrial gene co-expression patterns vary systematically across cancer types, potentially reflecting tumor-specific mitochondrial reprogramming. Based on significance filtering, a refined dataset was

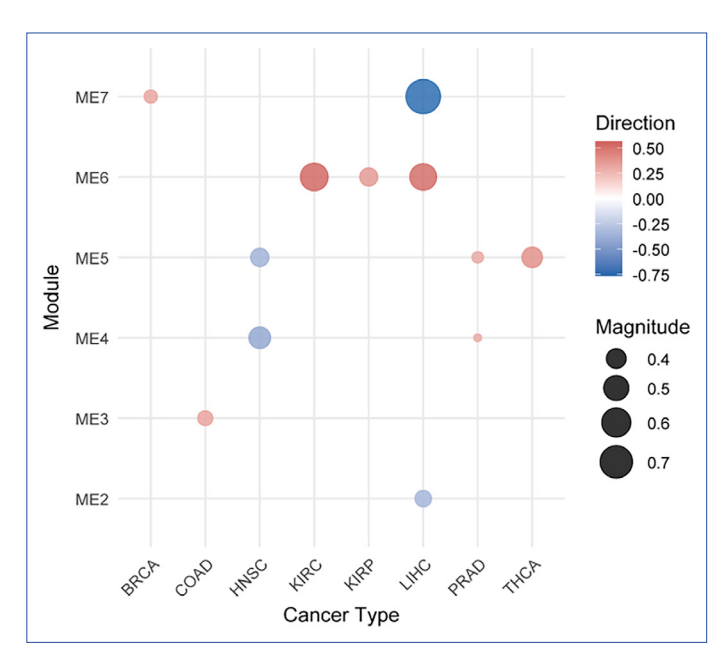


Figure 2. Module-cancer correlations. Bubble plot showing correlations between gene expression modules (ME2–ME7) and cancer types after significance filtering. Bubble size reflects the absolute correlation, while color indicates direction (red: positive, blue: negative).

generated comprising six modules (ME2 to ME7) and eight cancer types (BRCA, LIHC, COAD, KIRC, KIRP, HNSC, PRAD, and THCA). This subset included 544 genes and 4,269 tumor samples and was used for subsequent clustering, survival, and functional enrichment analyses. To provide a comprehensive overview, we included the full module–cancer correlation matrix, the module-level delta expression heatmap, and eigengene distributions across cancer types, shown in Appendix 3, 4, and 5, respectively.

Dimensionality reduction and clustering of module activity

To assess whether mitochondrial module activity could stratify tumors by type, we applied PCA, UMAP, and t-SNE to the expression profiles of 544 genes across 4,269 tumor samples. PCA accounted for a moderate portion of variance but yielded limited clustering performance for most cancer types (Fig. 3a). In contrast, both UMAP and t-SNE revealed clearer separation, with UMAP achieving the highest overall cluster quality and strongest within-type cohesion across several cancer types, notably PRAD, LIHC, and HNSC (Fig. 3b, c).

These findings indicate that non-linear dimensionality reduction techniques better capture the underlying mitochondrial expression patterns that differentiate tumor types.

Survival associations of mitochondrial modules

Univariate Cox proportional hazards analysis demonstrated significant associations between mitochondrial gene co-expression modules and overall survival across 7,202 tumor samples. Modules ME5, ME7, ME4, ME6, and ME2 were associated with improved prognosis, with hazard ratios ranging from approximately 0.40 to 0.79 (all adjusted p<0.001). Converse-

Table 2. Prognostic mitochondrial gene modules and their cancer-type-specific associations

| Module | Cancer | Survival effect (HR) |
|--------|------------------------------|-------------------------------|
| ME5 | HNSC (-), PRAD (+), THCA (+) | 0.40 (protective) |
| ME7 | BRCA (+), LIHC (-) | 0.46 (protective) |
| ME4 | HNSC (-), PRAD (+) | 0.47 (protective) |
| ME6 | KIRC (+), KIRP (+), LIHC (+) | 0.72 (protective) |
| ME2 | LIHC (-) | 0.79 (protective) |
| ME3 | COAD (+) | 1.25 (risk increasing) |
| Cancer | Modules | Survival effect (HR) |
| BRCA | ME7 (+) | 0.46 (protective) |
| COAD | ME3 (+) | 1.25 (risk increasing) |
| HNSC | ME4 (-), ME5 (-) | 0.47, 0.40 (protective) |
| KIRC | ME6 (+) | 0.72 (protective) |
| KIRP | ME6 (+) | 0.72 (protective) |
| LIHC | ME7 (-), ME2 (-), ME6 (+) | 0.46, 0.79, 0.72 (protective) |
| PRAD | ME4 (+), ME5 (+) | 0.47 ,0.40 (protective) |
| THCA | ME5 (+) | 0.40 (protective) |

Mitochondrial modules (ME2–ME7) showing significant associations with specific cancer types and corresponding hazard ratios (HR) from survival analysis are summarized. The top section lists each module and its correlated cancer types; the bottom section takes a cancer-centric view, indicating associated modules and their prognostic effects. Modules with HR < 1 indicate protective associations, while HR>1 suggests increased risk.

ly, ME3 showed a significant association with poorer survival (HR>1, adjusted p<0.001). These findings were consistently supported by Kaplan–Meier survival analyses (Fig. 4) and further quantified by module-specific hazard ratios calculated from scaled eigengene expression.

Functional signatures of mitochondrial modules

Each identified module represents a coordinated gene program reflecting distinct aspects of mitochondrial biology. Functional enrichment analyses revealed that modules are associated with specific mitochondrial processes as follows.

ME2 (Aminoacyl-tRNA and mitochondrial protein synthesis)

ME2 is enriched in mitochondrial aminoacyl-tRNA synthetases and components involved in mitochondrial translation, with pathway enrichments in Aminoacyl-tRNA biosynthesis, Mitochondrial tRNA Aminoacylation, and Translation. It also includes genes related to the TCA cycle, suggesting a link between protein synthesis and central carbon metabolism. Functionally, ME2 likely regulates mitochondrial translational capacity critical for bioenergetic demands. Its expression is negatively correlated with tumor presence and positively associated with better overall survival in liver hepatocellular carcinoma (LIHC), indicating that preserved mitochondrial translation supports favorable prognosis in metabolically active tumors. Disease association analysis highlights links to mitochondrial disorders such as lactic acidosis, reflecting mitochondrial dysfunction that may underlie LIHC metabolic reprogramming.

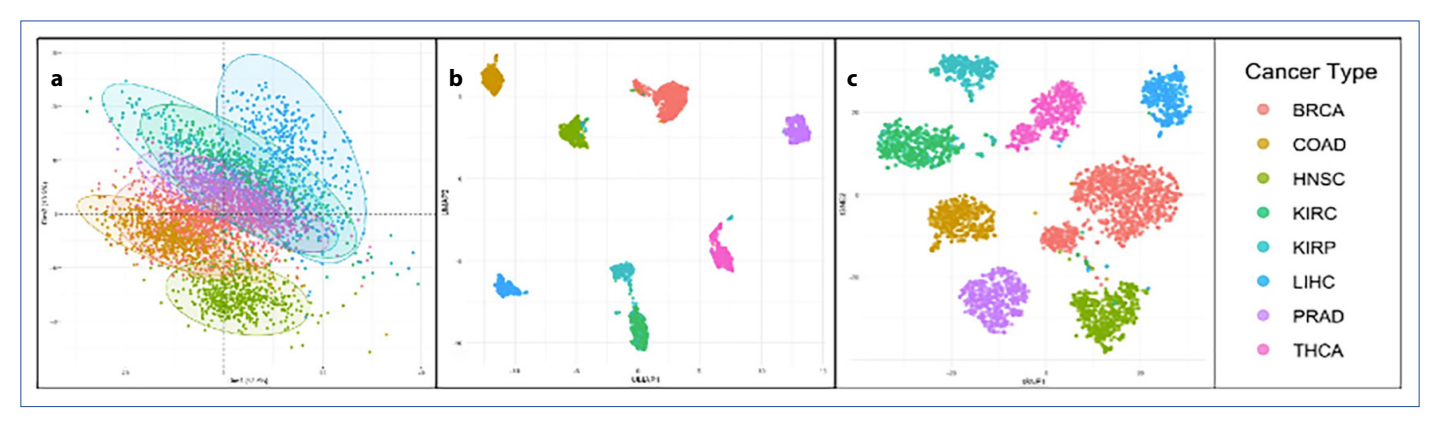


Figure 3. Dimensionality reduction analysis of module–trait relationships. (a) PCA, (b) UMAP, and (c) t-SNE plots illustrate the distribution of samples based on module eigengene expression profiles. Each point represents a sample, and colors correspond to different types of cancer as indicated in the legend. These visualizations highlight the clustering patterns and potential separability of cancer types based on module-level expression signatures.

PCA: Principal component analysis; UMAP: Uniform Manifold Approximation and Projection; t-SNE: t-Distributed Stochastic Neighbor Embedding.

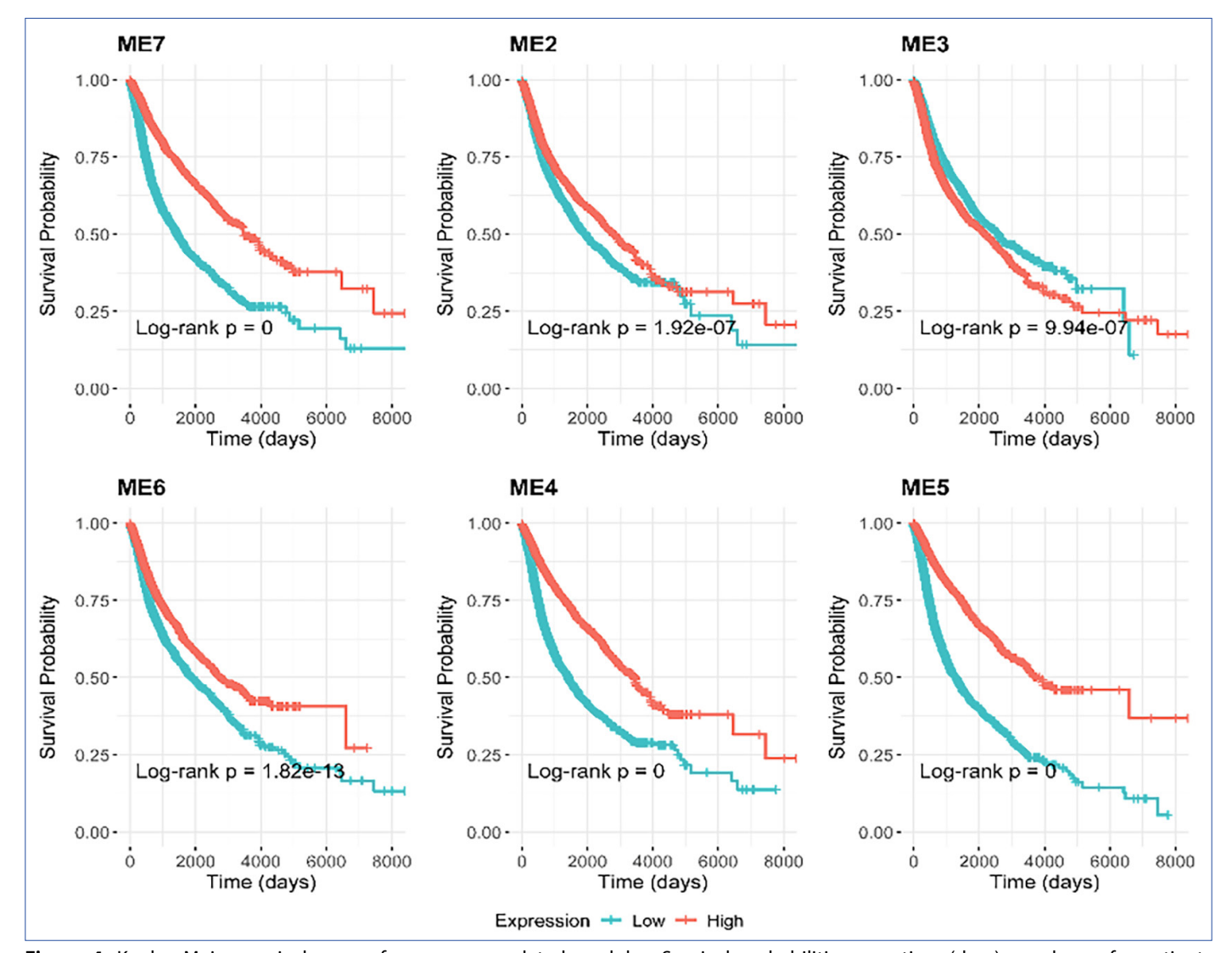


Figure 4. Kaplan-Meier survival curves for cancer correlated modules. Survival probabilities over time (days) are shown for patients stratified by high (red) versus low (blue) module expression. All differences between groups were statistically significant based on log-rank tests (adjusted p<0.001).

ME3 (Oxidative phosphorylation and mitochondrial translation initiation)

ME3 is enriched in genes related to mitochondrial translation initiation, oxidative phosphorylation (OXPHOS), and respiratory complex assembly, reflecting a coordinated bioenergetic program essential for ATP production. Key enriched pathways include Oxidative Phosphorylation, Respiratory Electron Transport, and Mitochondrial Translation Initiation. Clinically, ME3 expression positively correlates with tumor presence and poorer overall survival in colon adenocarcinoma (COAD), suggesting that elevated mitochondrial energy metabolism is associated with tumor aggressiveness. This module likely represents a mitochondrial bioenergetic signature contributing to cancer progression in COAD.

ME4 (Fatty acid β -oxidation and branched-chain amino acid catabolism)

ME4 is enriched for genes involved in mitochondrial fatty acid β -oxidation and branched-chain amino acid (BCAA) catabolism, with pathway enrichments highlighting lipid degradation, acyl-CoA metabolism, and peroxisomal lipid processing. Key enzymes in valine, leucine, and isoleucine degradation underscore ME4's role in maintaining mitochondrial energy homeostasis through versatile substrate utilization, especially under metabolic stress or nutrient scarcity.

ME5 (Apoptosis, mitochondrial dynamics, and calcium homeostasis)

ME5 is enriched in genes regulating intrinsic apoptosis, mitochondrial dynamics, and calcium transport, with key pathways including Apoptosis, Neurodegeneration, and Mitochondrial Calcium Ion Transport. This module likely coordinates mitochondrial quality control and stress responses. Clinically, ME5 expression is reduced in head and neck squamous cell carcinoma (HNSC), correlating with tumor presence and poorer prognosis, whereas in prostate adenocarcinoma (PRAD) and thyroid carcinoma (THCA), higher ME5 levels associated with better survival despite positive tumor correlation. These findings suggest a protective role of ME5 across cancers, with context-dependent transcriptional regulation reflecting mitochondrial integrity and apoptosis pathways.

ME6 (Lipid biosynthesis, Acyl-CoA metabolism, and amino acid conjugation)

ME6 is enriched in genes regulating fatty acid biosynthesis, acyl-CoA metabolism, glycine conjugation, and pathways related to detoxification and amino acid catabolism. Key pathways include Fatty Acid Beta-Oxidation, Peroxisome function, and Amino Acid Metabolism, indicating a role in lipid catabolism and mitochondrial–peroxisomal crosstalk. Clinically, ME6 expression positively correlates with tumor presence in kidney cancers (KIRC, KIRP) and liver hepatocellular carcinoma (LIHC), and associates with improved overall survival, suggesting a protective metabolic program that may limit tumor progression. This contrasts with modules

like ME7, characterized by downregulation of mitochondrial translation and negative correlation with tumors such as LIHC. While ME6 reflects an active metabolic state supporting fatty acid oxidation and detoxification linked to better prognosis, ME7 indicates mitochondrial dysfunction or repression of mitochondrial protein synthesis associated with more aggressive tumor behavior. Together, these differences highlight the complex and diverse mitochondrial adaptations across cancer types that shape tumor biology and patient outcomes.

ME7 (Ketone body metabolism, urea cycle, and sulfur amino acid turnover)

ME7 is enriched in genes involved in ketone body metabolism, urea cycle, and sulfur amino acid metabolism. Pathway annotations highlight ketone metabolism, nitrogen metabolism, and sulfur relay systems, suggesting roles in metabolic reprogramming during fasting or nutrient fluctuations, integrating nitrogen detoxification, energy substrate switching, and redox buffering. Functionally, ME7 is composed mainly of mitochondrial ribosomal proteins and oxidative phosphorylation components, reflecting a core mitochondrial translational and bioenergetic program essential for maintaining a balanced proteome, apoptosis regulation, and ATP production. Clinically, ME7 expression correlates positively with overall survival (HR=0.46), indicating preserved mitochondrial function may suppress tumor progression. ME7 shows cancer-type specific expression patterns: Upregulated in breast cancer (BRCA) and downregulated in liver hepatocellular carcinoma (LIHC). These findings may reflect tissue-specific metabolic reprogramming. In BRCA tumors, the retention of mitochondrial translation and apoptotic signaling is associated with better prognosis, whereas LIHC exhibits metabolic dedifferentiation and hypoxic adaptation. The loss of ME7 module expression in LIHC further supports a shift toward aggressive tumor phenotypes. Downregulation of ME7 in LIHC mirrors disruption of mitochondrial metabolic pathways including amino acid and nitrogen metabolism, supporting aggressive tumor phenotypes. Conversely, ME7 upregulation in BRCA aligns with preserved mitochondrial function and metabolic flexibility, promoting controlled tumor growth and apoptosis. Overall, ME7 represents a mitochondria-centered tumor suppressive module whose context-dependent expression is prognostically informative, underscoring the interplay between mitochondrial translation, apoptosis, and metabolic adaptation in cancer biology.

Discussion

Our integrative analysis of mitochondrial-related gene expression modules across multiple cancer types reveals distinct module-cancer specificity patterns with significant prognostic implications as summarized in Table 2. Modules ME2, ME4, ME5, ME6, and ME7 generally demonstrate protective effects on overall survival, whereas ME3 shows a risk-increasing effect, highlighting the heterogeneous roles

of mitochondrial functions in cancer progression. Notably, ME2 exhibits a strong protective association uniquely in liver hepatocellular carcinoma (LIHC), consistent with its role in mitochondrial aminoacyl-tRNA synthetase function and bioenergetic regulation. ME3, conversely, correlates positively with tumor presence and worse prognosis specifically in colon adenocarcinoma (COAD), reflecting heightened oxidative phosphorylation activity potentially driving tumor aggressiveness. Modules ME4 and ME5 show complex, cancer-specific correlation directions, protective in some cancers (e.g., HNSC) but positively correlated in others (e.g., PRAD, THCA), indicating context-dependent mitochondrial pathway engagement. Modules ME6 and ME7 also display strong protective effects with positive correlations in kidney cancers (KIRC, KIRP) and breast cancer (BRCA), respectively, supporting the notion that mitochondrial functional states may influence survival in a tumor-type-specific manner.

Overall, our results emphasize the potential of mitochondrial functional modules as robust prognostic biomarkers and promising therapeutic targets across diverse cancer types. For instance, ME2's strong protective association specifically in liver hepatocellular carcinoma (LIHC) highlights how preserving mitochondrial translational capacity may suppress tumor progression in metabolically demanding tumors. Conversely, the risk-increasing profile of ME3 in (COAD) suggests that elevated mitochondrial oxidative phosphorylation activity contributes to tumor aggressiveness in this cancer type. These cancer-specific patterns suggest that mitochondrial dysfunction and metabolic rewiring may vary across tumors, reflecting distinct bioenergetic adaptations. This modular perspective may inform metabolic precision oncology, where therapeutic strategies can be tailored based on the dominant mitochondrial module dysregulated in a patient's tumor. Such an approach may enhance treatment efficacy by addressing cancer-specific metabolic dependencies, as exemplified by ME2-associated modules in LIHC potentially benefiting from therapies that restore mitochondrial translation and bioenergetics, while ME3-associated pathways in COAD might be targeted by inhibitors of oxidative phosphorylation. Therefore, integrating mitochondrial module profiling into clinical decision-making offers a promising avenue for developing more effective, personalized cancer treatments grounded in tumor metabolic phenotyping.

Furthermore, when stratifying tumors by their estimated metabolic phenotypes, we observed a striking pattern: Nearly all tumors classified as HGLO (High Glycolysis, Low OXPHOS (Oxidative Phosphorylation)— meaning they rely mainly on glycolysis and have suppressed mitochondrial respiration—belonged to the subset of cancers that showed no significant correlation with mitochondrial gene modules. In contrast, all tumors classified as HGHO (High Glycolysis, High OXPHOS)—which maintain both glycolytic and mitochondrial activity— were exclusively found among cancers with strong and consistent correlations with mitochondrial modules.

This distribution aligns with prior pan-cancer metabolic classifications [28], and suggests that mitochondrial module engagement may be shaped by the tumor's dominant metabolic strategy. Specifically, tumors with suppressed oxidative phosphorylation (HGLO) may show lower activity of mitochondrial gene modules, which can reduce ATP production and alter redox balance, explaining the lack of correlation. Conversely, tumors with active mitochondrial metabolism (HGHO) rely more on mitochondrial energy production and biosynthetic pathways, resulting in enhanced energy production and robust module engagement. These findings support the view that mitochondrial module expression may be both cancer-type specific and metabolically contextual and highlight the importance of integrating metabolic phenotyping into mitochondrial biomarker interpretation.

Our findings align with the evolving paradigm of mitochondria as dynamic cancer regulators. While early studies focused on the Warburg effect, we now recognize their pleiotropic roles in metabolic reprogramming, ROS signaling, and apoptosis [7, 13, 29, 30]. Notably, our results supports that mitochondrial adaptations are highly context-dependent across tumor types [13, 31]. These modules—particularly in translation and bioenergetics—may explain observed therapeutic resistance [7, 32], suggesting that targeting mitochondrial plasticity requires personalized approaches. Consequently, stratifying tumors by mitochondrial module expression profiles may thus provide a framework for metabolic subtyping and inform therapeutic strategies targeting mitochondrial vulnerabilities. Although key mitochondrial modules with prognostic and subtype-specific relevance were identified, functional validation is needed to clarify their causal roles. Integrating additional data such as mutations, epigenetics, and metabolomics could deepen mechanistic insights. Future studies should assess the potential of these modules as predictive biomarkers for patient stratification and therapies targeting metabolic vulnerabilities.

Interestingly, the cancer-type-specific behavior of mitochondrial modules may reflect a form of adaptive pleiotropy, a concept previously described in microbial systems [33–35]. In such contexts, early adaptive mutations often occur in global regulators, leading to broad transcriptomic shifts that influence multiple traits simultaneously [36]. Analogous regulatory dynamics may underlie the divergent prognostic roles of modules like ME2 and ME7 across tumor types. The lack of module association in HGLO tumors may further support this interpretation, consistent with stress-induced mitochondrial suppression. These observations suggest that mitochondrial modules may operate within regulatory architectures that favor coordinated multi-trait adaptation, reinforcing their role as context-sensitive hubs in cancer evolution [37-39]. In summary, our findings support the concept of adaptive mitochondrial modules that 'go with the flow' of cancer-specific metabolic rewiring, highlighting their potential as context-sensitive biomarkers and therapeutic targets.

Online Appendix Files: https://jag.journalagent.com/ijmb/abs_files/IJMB-32656/IJMB-32656_(3)_IJMB-32656_Appendix.pdf

Informed Consent: Informed consent was obtained from all participants.

Conflict of Interest Statement: The authors have no conflicts of interest to declare.

Funding: The authors declared that this study received no financial support.

Use of AI for Writing Assistance: AI tools were used only for language editing and technical refinement.

Peer-review: Externally peer-reviewed.

References

- 1. Huitzil S, Huepe C. Life's building blocks: The modular path to multiscale complexity. Front Syst Biol 2024;4:1417800. [CrossRef]
- Daves J. Exploring biological systems: Complexity, dynamics, and interact. Available at: https://www.scholarsresearchlibrary.com/articles/exploring-biological-systems-complexity-dynamics-and-interactions-108015.html. Accessed Aug 29, 2025.
- 3. Axenie C, Bauer R, Martínez MR. The multiple dimensions of networks in cancer: A perspective. Symmetry 2021;13(9):1559. [CrossRef]
- 4. Alon U. Network motifs: Theory and experimental approaches. Nat Rev Genet. 2007;8(6):450–61. [CrossRef]
- 5. Kitano H. Systems biology: A brief overview. Science 2002;295(5560):1662–4. [CrossRef]
- 6. Tyson JJ, Chen KC, Novak B. Sniffers, buzzers, toggles and blinkers: Dynamics of regulatory and signaling pathways in the cell. Curr Opin Cell Biol 2003;15(2):221–31. [CrossRef]
- 7. Weinberg SE, Chandel NS. Targeting mitochondria metabolism for cancer therapy. Nat Chem Biol 2015;11(1):9–15. [CrossRef]
- 8. Zong WX, Rabinowitz JD, White E. Mitochondria and cancer. Mol Cell 2016;61(5):667–76. [CrossRef]
- Porporato PE, Filigheddu N, Pedro JMBS, Kroemer G, Galluzzi L. Mitochondrial metabolism and cancer. Cell Res 2018;28(3):265–80. [CrossRef]
- 10. Cantó C. Mitochondrial dynamics: Shaping metabolic adaptation. Int Rev Cell Mol Biol 2018;340:129–67. [CrossRef]
- 11. Nunnari J, Suomalainen A. Mitochondria: in sickness and in health. Cell 2012;148(6):1145–59. [CrossRef]
- 12. Vyas S, Zaganjor E, Haigis MC. Mitochondria and cancer. Cell 2016;166(3):555–66. [CrossRef]
- 13. Wallace DC. Mitochondria and cancer. Nat Rev Cancer 2012;12(10):685–98. [CrossRef]
- 14. Zhao Q, Wang J, Levichkin IV, Stasinopoulos S, Ryan MT, Hoogenraad NJ. A mitochondrial specific stress response in mammalian cells. EMBO J 2002;21(17):4411–9. [CrossRef]
- 15. Asghar U, Witkiewicz AK, Turner NC, Knudsen ES. The history and future of targeting cyclin-dependent kinases in cancer therapy. Nat Rev Drug Discov 2015;14(2):130–46. [CrossRef]
- 16. Hanahan D, Weinberg RA. Hallmarks of cancer: The next generation. Cell 2011;144(5):646–74. [CrossRef]
- 17. Kitano H. Cancer as a robust system: Implications for anticancer therapy. Nat Rev Cancer 2004;4(3):227–35. [CrossRef]

18. Malumbres M. Cyclin-dependent kinases. Genome Biol 2014;15(6):122. [CrossRef]

- 19. Shapiro Gl. Cyclin-dependent kinase pathways as targets for cancer treatment. J Clin Oncol 2006;24(11):1770–83. [CrossRef]
- 20. Vasan K, Werner M, Chandel NS. Mitochondrial metabolism as a target for cancer therapy. Cell Metab 2020;32(3):341–52. [CrossRef]
- 21. The Cancer Genome Atlas Program (TCGA) NCI. 2022. Available at: https://www.cancer.gov/ccg/research/genome-sequencing/tcga. Accessed Sep 16, 2025.
- 22. Tomczak K, Czerwińska P, Wiznerowicz M. The Cancer Genome Atlas (TCGA): An immeasurable source of knowledge. Contemp Oncol (Pozn) 2015;19(1A):A68–77. [CrossRef]
- 23. Grossman RL, Heath AP, Ferretti V, Varmus HE, Lowy DR, Kibbe WA, et al. Toward a shared vision for cancer genomic data. N Engl J Med 2016;375(12):1109–12. [CrossRef]
- 24. Evangelista JE, Xie Z, Marino GB, Nguyen N, Clarke DJB, Ma'ayan A. Enrichr-KG: bridging enrichment analysis across multiple libraries. Nucleic Acids Res 2023;51(W1):W168–79. [CrossRef]
- 25. Li R, Qu H, Wang S, Wei J, Zhang L, Ma R, et al. GDCRNATools: An R/Bioconductor package for integrative analysis of IncRNA, miRNA and mRNA data in GDC. Bioinformatics 2018;34(14):2515–7. [CrossRef]
- 26. Rath S, Sharma R, Gupta R, Ast T, Chan C, Durham TJ, et al. MitoCarta3.0: An updated mitochondrial proteome now with sub-organelle localization and pathway annotations. Nucleic Acids Res 2021;49(D1):D1541–7. [CrossRef]
- 27. Langfelder P, Horvath S. WGCNA: An R package for weighted correlation network analysis. BMC Bioinformatics 2008;9:559. [CrossRef]
- 28. Hoadley KA, Yau C, Hinoue T, Wolf DM, Lazar AJ, Drill E, et al. Cell-of-origin patterns dominate the molecular classification of 10,000 tumors from 33 types of cancer. Cell 2018;173(2):291–304.e6.
- 29. Vander Heiden MG, Cantley LC, Thompson CB. Understanding the Warburg effect: The metabolic requirements of cell proliferation. Science 2009;324(5930):1029–33. [CrossRef]
- 30. Warburg O. On the origin of cancer cells. Science 1956;123(3191):309–14. [CrossRef]
- 31. Chandel NS. Evolution of mitochondria as signaling organelles. Cell Metab 2015;22(2):204–6. [CrossRef]
- 32. Liberti MV, Locasale JW. The Warburg effect: How does it benefit cancer cells? Trends Biochem Sci 2016;41(3):211–8. [CrossRef]
- 33. Deyell M, Opuu V, Griffiths AD, Tans SJ, Nghe P. Global regulators enable bacterial adaptation to a phenotypic trade-off. iScience 202;28(1):111521. [CrossRef]
- 34. Wagner GP, Zhang J. The pleiotropic structure of the genotype-phenotype map: The evolvability of complex organisms. Nat Rev Genet 2011;12(3):204–13. [CrossRef]
- 35. Couce A. Regulatory networks may evolve to favor adaptive foresight. PLoS Biol 2024;22(12):e3002922. [CrossRef]
- 36. Kinsler G, Geiler-Samerotte K, Petrov D. A genotype-phenotype-fitness map reveals local modularity and global pleiotropy of adaptation. bioRxiv 2020;2020: 2020.06.25.172197. [CrossRef]

- 37. Avolio R, Matassa DS, Criscuolo D, Landriscina M, Esposito F. Modulation of mitochondrial metabolic reprogramming and oxidative stress to overcome chemoresistance in cancer. Biomolecules 2020;10(1):135. [CrossRef]
- 38. Pendleton KE, Wang K, Echeverria GV. Rewiring of mitochondrial metabolism in therapy-resistant cancers:
- Permanent and plastic adaptations. Front Cell Dev Biol 2023;11:1254313. [CrossRef]
- 39. Berner MJ, Wall SW, Echeverria GV. Deregulation of mitochondrial gene expression in cancer: Mechanisms and therapeutic opportunities. Br J Cancer 2024;131(9):1415–24. [CrossRef]